Journal of Power Sources 195 (2010) 4247–4251

Contents lists available at ScienceDirect

Journal of Power Sources

journal homepage: www.elsevier.com/locate/jpowsour

Short communication

Performance of an annular solid-oxide fuel cell micro-stack array operating in single-chamber conditions

Mingliang Liu[a], Zhe Lü[a,*], Bo Wei[a], Xiqiang Huang[a], Yaohui Zhang[a], Wenhui Su[a,b]

[a] Center for Condensed Matter Science and Technology, Department of Physics, Harbin Institute of Technology, Harbin 150080, China
[b] International Center for Material Physics, Chinese Academy of Sciences, Shenyang 110015, China

ARTICLE INFO

Article history:
Received 5 November 2009
Received in revised form
23 December 2009
Accepted 29 December 2009
Available online 13 January 2010

Keywords:
Solid-oxide fuel cell
Single-chamber conditions
Micro-stack
Annular array configuration

ABSTRACT

An annular micro-stack array consisting of four fuel cells has been fabricated and operated successfully in single-chamber conditions using a nitrogen-diluted oxygen–methane mixture as the operating gas. The single cells consist of a state-of-the-art porous NiO/Y_2O_3-stabilized ZrO_2 (YSZ) anode support, a YSZ electrolyte membrane and a modified $La_{0.7}Sr_{0.3}MnO_3$ (LSM) cathode. The annular configuration of the array is favorable for utilizing the heating effect. The maximum power output of the annular stack decreases with increasingCH_4/O_2 ratio. Its performance increases with increasing CH_4 flow rate and decreases with increasing N_2 flow rate. The power output of the stack is ~380 mW at $CH_4/O_2 = 1$ and an N_2 flow rate of 100 sccm and the average maximum power density of each cell is ~190 mW cm^{-2}. The average performance of each cell in the annular micro-stack array is higher than that of an additional single cell placed next to the stack.

1. Introduction

Recently, single-chamber solid-oxide fuel cells (SC-SOFCs) have attracted a great deal of attention [1]. This is mainly due to the need for new portable equipment capable of providing higher energy density and higher specific energy [2]. As compared with conventional SOFCs, SC-SOFCs usually operate in a diluted gas mixture of fuel and oxidant. This typical characteristic enables an SC-SOFC stack to have the advantages of being sealant-free and having rapid start-up and improved thermal and mechanical shock resistance [1].

The operating principle of SC-SOFCs is based on the catalytic selectivity of the electrodes towards the fuel/oxidant gas mixture, which accordingly generates an electromotive force (EMF) across the cell. For example, in a methane–oxygen mixture, CH_4 is partly oxidized to a syngas of CO and H_2 at the anode, which is then further electrochemically oxidized to CO_2 and H_2O. The reactions are

$$CH_4 + \tfrac{1}{2}O_2 \rightarrow CO + 2H_2 \quad (1)$$

$$H_2 + O^{2-} \rightarrow H_2O + 2e^- \quad (2)$$

$$CO + O^{2-} \rightarrow CO_2 + 2e^- \quad (3)$$

Oxygen is electrochemically reduced at the cathode:

$$\tfrac{1}{2}O_2 + 2e^- \rightarrow O^{2-} \quad (4)$$

In the last decade, higher power densities have been obtained for SC-SOFCs [3–6]. At the same time, not only electrolyte-supported SC-SOFC modules [7–9] but also stacks consisting of several cells have been fabricated and operated successfully in single-chamber conditions [10–16]. Some stack designs for SC-SOFCs have been presented, and good results have been obtained with them. Shao et al. [10] fabricated a thermally self-sustained micro-stack that generated an open-circuit voltage (OCV) of 1.44 V and a maximum power of about 350 mW. The temperature of the stack was maintained by using the heating effect of the reaction. The addition of a porous layer consisting of $Ru + CeO_2$ significantly enhanced the exothermic partial oxidation of propane at the anode, which successfully sustained the operation of the stack with an anode-facing-anode configuration at ~580 °C.

In our previous work [16], we fabricated anode-facing-cathode dual-cell stacks with various distances between the cells. The effect of this distance on the performance of a single cell and the stack was investigated. While the distance appeared to have no significant effect on the cathode of cell 2 facing the distance between the two cells, the power output of cell 2 was a bit higher than that of cell 1. This may have been caused by the heating effect from the exothermic reaction at the anode of cell 1. In order to utilize this heating effect further for improving the performance of an SC-SOFC stack, a new configuration with the cells arrayed annularly is proposed here. In this study, a novel annular micro-stack array con-

* Corresponding author. Tel.: +86 461 86418420; fax: +86 461 86418420.
E-mail address: lvzhe@hit.edu.cn (Z. Lü).

0378-7753/$ – see front matter © 2010 Elsevier B.V. All rights reserved.
doi:10.1016/j.jpowsour.2009.12.124

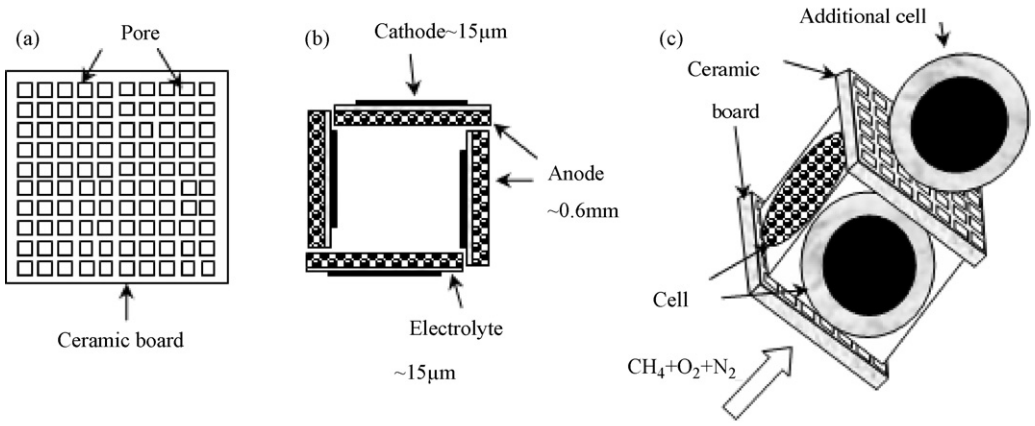

Fig. 1. The schematic diagram of the ceramic board and four-cell stack (a) the ceramic board, (b) the series-wound stack and (c) 3D views of the stack.

sisting of four cells has been fabricated and operated successfully in CH_4–O_2–N_2 mixtures. The effect of the gas composition and flow rate on the performance of the stack has also been investigated.

2. Experimental

2.1. Single-cell fabrication

Anode-supported fuel cells consisting of Ni/YSZ anodes, YSZ membranes and modified $La_{0.7}Sr_{0.3}MnO_3$ (LSM) cathodes were fabricated. The anode powder was prepared by mixing YSZ (TZ-8Y, Tosoh Corp., Japan), NiO and flour at a weight ratio of 5:5:2. Dense YSZ membranes were fabricated on the anode substrates using a slurry spin-coating method. The bi-layer of YSZ and anode substrate was co-sintered at 1400 °C for 4 h. LSM paste was painted on the electrolyte membrane. Details of the procedure for preparing the fuel cells can be found elsewhere [11,15]. The porous cathodes were impregnated with a 3 mol L^{-1} $Sm_{0.2}Ce_{0.8}(NO_3)_x$ solution and heat-treated at 850 °C for 1 h to improve the cathode performance [17]. The active area of the cathode was 0.5 cm^2.

2.2. Micro-stack assembly

The anode substrates were reduced in hydrogen at 700 °C before assembly. This reduction of the anode used the conventional dual-chamber SOFC configuration to avoid the reducing the cathodes. The electrode surfaces were covered with a thin layer of Ag paste (DAD-87) as the current collector and the cells were then connected to the test instruments with silver wires.

Fig. 1 shows a schematic diagram of the ceramic board and the array of cells. A piece of lightweight dichroite ceramic board (Fig. 1a) with many square holes (side length ~1 mm) was used as the support for assembling the stack. In order to fix the cells in place, the surface of the ceramic board was fluted. The four cells were arrayed annularly in series (Fig. 1b). The gas flow was in parallel with the cells. An additional single cell was also assembled using another piece of ceramic board behind the four-cell stack along the direction of the gas flow (Fig. 1c).

2.3. Electrochemical characterization

The performance of the stack and single cell was tested in a quartz tube (inner and outer diameters of ~21.6 mm and 24.6 mm, respectively). The gas mixture consisted of methane as fuel, oxygen as oxidant and nitrogen as inert diluting gas. The flow rate of these gases and the ratio of methane to oxygen were controlled by mass-flow controllers (MFCs, D08-4D/2M, Seven-Star Huachuang, China). The *I–V* performance and ac impedance spectra of the stack were measured by a Solartron SI 1287 electrochemical interface and a Solartron SI 1260 impedance gain/phase analyzer. The frequency was changed from 0.1 Hz to 91 kHz for measurements of the impedance spectra.

3. Results and discussion

Fig. 2 shows the discharge curves of the four-cell stack for various compositions of the gas mixture. The total flow rate of CH_4 and O_2 is 200 sccm and the flow rate of N_2 is 200 sccm. The OCVs of the cells in the stack have almost the same value of ~3.3 V, and the maximum power output decreases with increasing CH_4 content. The maximum power output is close to 300 mW at $CH_4/O_2 = 1$. However, the *I–V* curve shows serious concentration polarization at higher current densities. This behavior is due to the formation of more of the total oxidation products of CO_2 and H_2O, in particular for the four inner electrodes. The annular configuration of the stack array is helpful for keeping the four cells hotter. In other words, the inner electrodes not only take up a smaller space, but they also have a higher temperature. So the inner electrodes need more of the gas mixture to take part in the electrode reactions at a higher rate. At the same time, the reaction products should be removed from the inner electrodes in good time. If insufficient reaction gas is fed in or the products are not removed in time, concentration polarization

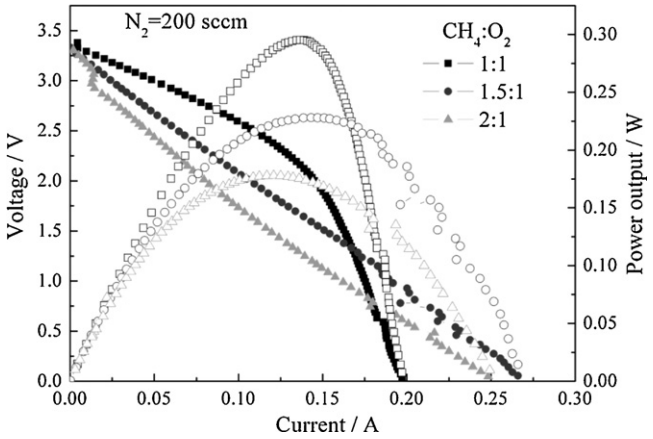

Fig. 2. *I–V* and *I–P* curves of the stack for various CH_4/O_2 ratios at 700 °C (the flow rate of $CH_4 + O_2$ is 200 sccm).

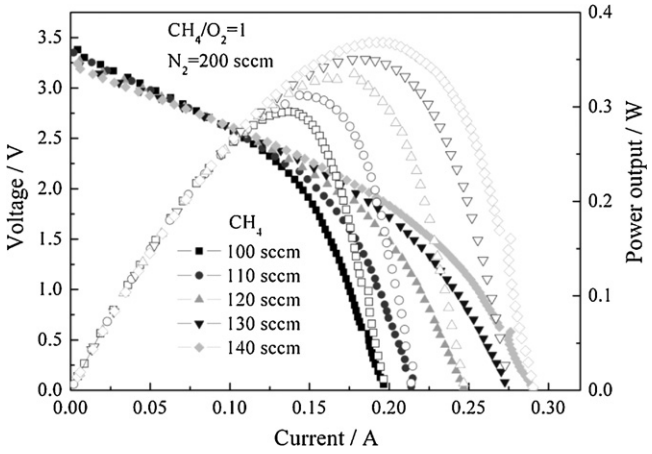

Fig. 3. *I–V* and *I–P* curves of the stack for various flow rates of CH_4 at 700 °C.

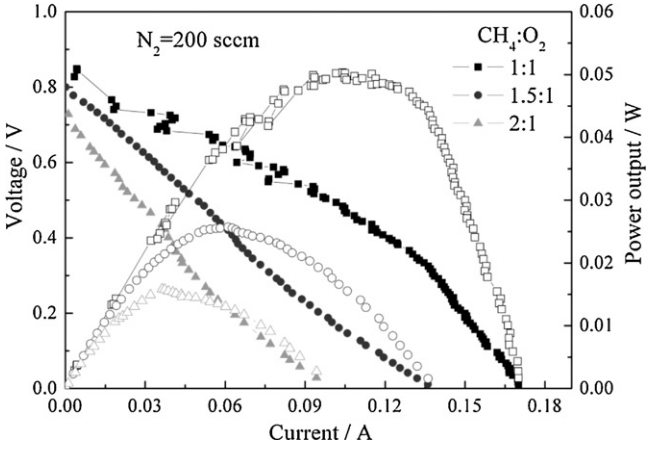

Fig. 5. *I–V* and *I–P* curves of the additional single cell for various CH_4/O_2 ratios at 700 °C.

will occur. At the same time, the *I–V* curves at $CH_4/O_2 = 1.5$ and 2 are not as stable as the *I–V* curve at $CH_4/O_2 = 1$, due to the lack of O_2. So a higher flow rate of CH_4 and O_2 is needed in order to feed in enough reaction gas and improve the flow rate of the products. Fig. 3 shows the *I–V* and *I–P* curves of the stack for various flow rates of CH_4 at $CH_4/O_2 = 1$. The peak power output of the stack increases with increasing gas-flow rate. The maximum power outputs are 295, 313, 335, 350 and 368 mW at CH_4 flow rates of 100, 110, 120, 130 and 140 sccm, respectively. The concentration polarization is also mitigated as the CH_4 flow rate increases. The residence time, which is an important parameter in SC-SOFCs, is shortened with increasing gas-flow rates. The fuel utilization also decreases with decreasing residence time [18]. Therefore, a moderate CH_4 flow rate should be used in this stack to obtain both high power output and acceptable fuel utilization.

At the same time, the N_2 flow rate also has an influence on the residence time. Fig. 4 shows the *I–V* and *I–P* curves of the stack for various flow rates of N_2 at $CH_4/O_2 = 1$. The OCV of the stack increases as the N_2 flow rate is increased. However, the peak power output of the stack decreases with increasing N_2 flow rate. The maximum power outputs are 380, 368, 308 and 243 mW at N_2 flow rates of 100, 200, 300 and 400 sccm, respectively. The average maximum power density of each cell is ~190 mW cm^{-2} at an N_2 flow rate of 100 sccm. A higher flow rate of N_2 will carry heat from the cell, thus reducing its temperature. So the OCV is highest at an N_2 flow rate of 400 sccm and the power output is highest at an N_2 flow rate of 100 sccm. At higher flow rates, the *I–V* curve also shows serious concentration polarization at higher current densities. This is

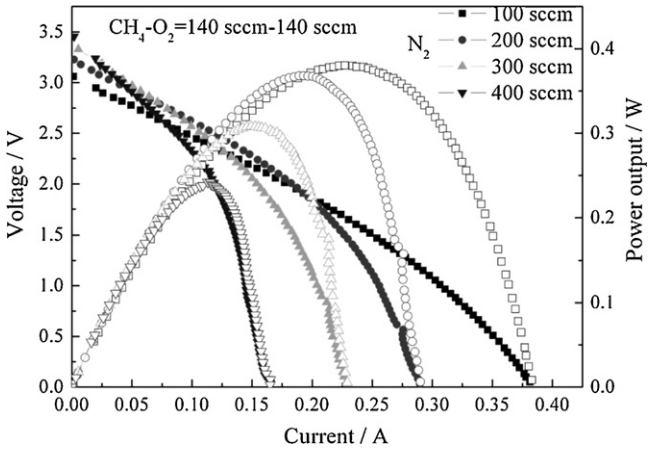

Fig. 4. *I–V* and *I–P* curves of the stack for various flow rates of N_2 at 700 °C.

because a higher N_2 flow rate removes a lot of reaction gas (CH_4 and O_2) from the electrodes without reaction. The electrodes cannot obtain enough reaction gas because it is diluted by N_2 in single-chamber conditions. The performance of the stack at an N_2 flow rate of 100 sccm is the highest because the cells obtain enough fuel and oxygen, and the residence time is long. This long residence time could increase the fuel utilization [18], which can be estimated by the current efficiency $\varepsilon = I/I_F$ where I and I_F are the actual current and the current calculated for 100% fuel conversion, respectively [19]. I_F can be calculated by combining Eqs. (1)–(3), the fuel-flow rate and Faraday's law. The highest current efficiency of the stack was estimated to be ~2.4%. The average current efficiency of a single cell (~0.6%) is a little higher than that of the dual-cell stack design (~0.5%) in our previous results [11], probably due to the heating effect. However, the average power density is lower than that of the dual-cell stack design, which has better operating conditions than those of the annular stack array.

In order to increase the fuel utilization and analyze the surplus gas, an additional single cell was arranged on another piece of ceramic board behind the four-cell stack along the direction of the gas flow. Fig. 5 shows the *I–V* and *I–P* curves of this additional single cell for various CH_4/O_2 ratios. Its performance increases as the CH_4/O_2 ratio is decreased. The performances of the cell at $CH_4/O_2 = 2$ and 1.5 are much worse than that at $CH_4/O_2 = 1$, the change being larger than that in Fig. 2. The power density of the cell is lower than the average value for each cell in the stack. This indicates that the condition of the gas in the additional cell is bad, especially in oxygen-poor mixtures, and the actual temperature of the cell is probably lower than that of a cell in the annular stack array. Fig. 6 shows the *I–V* and *I–P* curves of the additional single cell for various CH_4 flow rates at $CH_4/O_2 = 1$. Compared with Fig. 3, the power output of the single cell increases only slightly as the CH_4 flow rate increases. This suggests that the amount of gas coming from the stack, in particular from its square area, increases only slightly or that the cell has obtained enough reaction gas. If the gas coming from the stack changes a little, the increased amount of gas is almost used up by the electrodes of the stack. The power output of the stack increases with the CH_4 flow rate, indicating that the consumption of CH_4 should be increased. Fig. 7 shows the *I–V* and *I–P* curves of the single cell for various flow rates of N_2 at $CH_4/O_2 = 1$. Both the OCV and the power output of the additional single cell increase with the N_2 flow rate. The additional single cell obtains more reaction gases from the higher N_2 flow rate. However, the performance of the additional single cell falls a little at an N_2 flow rate of 400 sccm. For a moderate total gas-flow rate, some heat coming from the stack can increase the temperature and improve

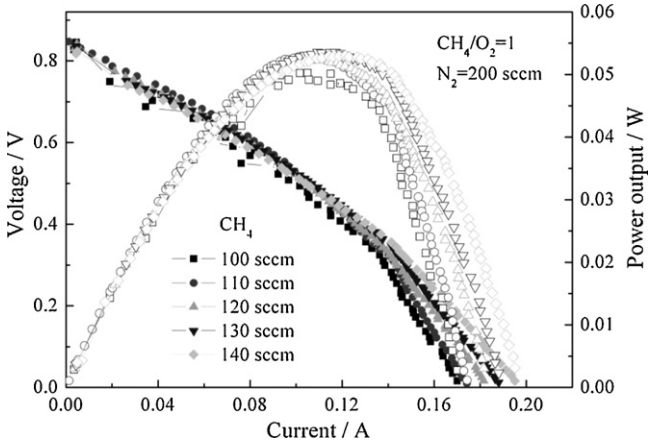

Fig. 6. *I–V* and *I–P* curves of the additional single cell for various flow rates of CH_4 at 700 °C.

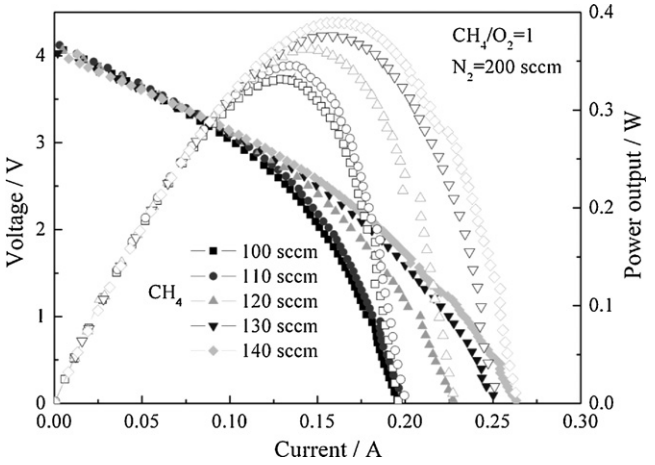

Fig. 8. *I–V* and *I–P* curves of the five-cell stack for various flow rates of CH_4 at 700 °C.

the performance of the additional cell, but under the highest flow rate, the gas may remove some heat not only from the stack but also from the additional single cell. The annular configuration of the array can indeed increase the use of the heating effect because the power density of the additional single cell is lower than the average power density of each cell in the stack. At the same time, the *I–V* and *I–P* curves, shown in Figs. 5–7, are not stable because the gas flow from the annular stack array is unstable. The fuel utilization increases ~0.25% due to the addition of the single cell.

Fig. 8 shows the *I–V* and *I–P* curves of the five-cell stack for various flow rates of CH_4 at $CH_4/O_2 = 1$. This stack consists of the four-cell annular stack array and the additional single cell, which is behind the stack. The maximum power outputs are 330, 345, 360, 376 and 390 mW at CH_4 flow rates of 100, 110, 120, 130 and 140 sccm, respectively. The average maximum current of the five-cell stack is higher than that of the additional single cell, but lower than that of the four-cell annular stack array, due to the difference in the inner resistances of the single cells. The annular stack array can improve the utilization of the heating effect. If a coaxial annular array is used, the stack can contain more cells and further utilize the heat to improve the performance of the cells. A coaxial cylindrical-type stack can also be fabricated using tubular SOFCs with various diameters [20].

4. Conclusions

An annular micro-stack array consisting of four fuel cells has been fabricated and operated successfully in CH_4–O_2–N_2 mixtures. The annular configuration of the array is favorable for the use of the heating effect. The power output of the stack is ~380 mW at N_2 flow rates of 100 sccm and the average maximum power density of each cell is ~190 mW cm^{-2}. The average performance of each cell in the annular stack array is higher than that of an additional single cell next to the stack. This additional cell was used to analyze the surplus gas and increase the fuel utilization. If several coaxial annular arrays are fabricated, they can not only contain more cells to obtain a high OCV and power output, but can also cause a distinct improvement in the utilization of the reaction heat.

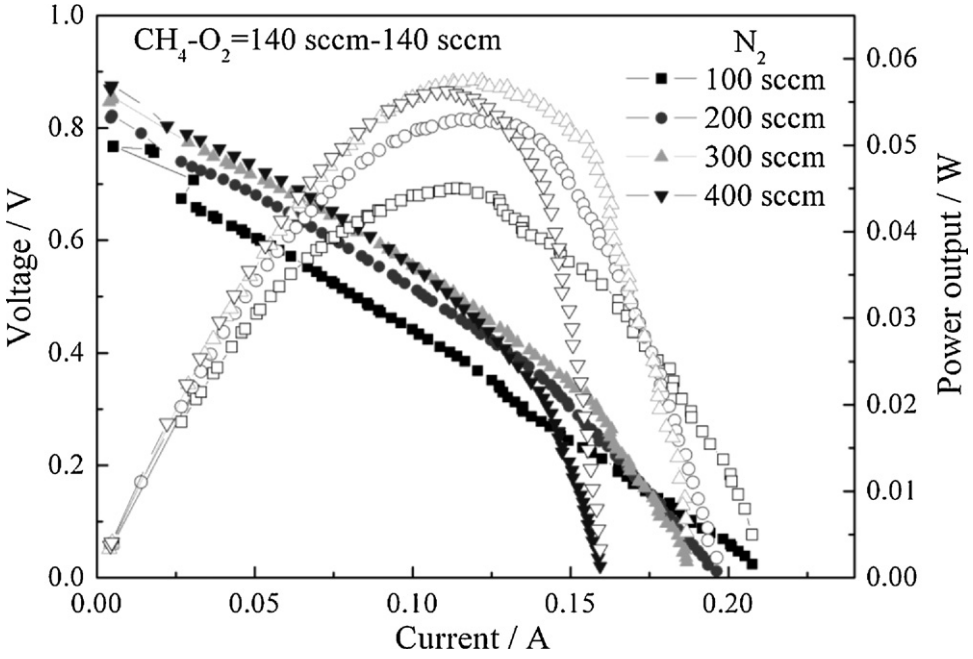

Fig. 7. *I–V* and *I–P* curves of the additional single cell for various flow rates of N_2 at 700 °C.

Acknowledgement

This research was supported by the Ministry of Science and Technology of China (2007AA05Z139).

References

[1] M. Yano, A. Tomita, M. Sano, T. Hibino, Solid State Ionics 177 (2007) 3351–3359.
[2] C.K. Dyer, J. Power Sources 106 (2002) 31–34.
[3] T. Hibino, A. Hashimoto, T. Inoue, J. Tokuno, S. Yoshida, M. Sano, Science 288 (2000) 2031–2033.
[4] T. Hibino, A. Hashimoto, M. Yano, M. Suzuki, S. Yoshida, M. Sano, J. Electrochem. Soc. 149 (2002) A133–A136.
[5] T. Suzuki, P. Jasinski, V. Petrovsky, H.U. Anderson, F. Dogan, J. Electrochem. Soc. 152 (2005) A527–A531.
[6] Z. Shao, J. Mederos, W.C. Chueh, S.M. Haile, J. Power Sources 162 (2006) 589–596.
[7] T. Hibino, K. Ushiki, Y. Kuwahara, Solid State Ionics 91 (1996) 69–74.
[8] T. Suzuki, P. Jasinski, H.U. Anderson, F. Dogan, Electrochem. Solid State Lett. 7 (2004) A391–A393.
[9] B.E. Buergler, M. Ochsner, S. Vuillemin, L.J. Gauckler, J. Power Sources 171 (2007) 310–320.
[10] Z. Shao, S.M. Haile, J. Ahn, P.D. Ronney, Z. Zhan, S.A. Barnett, Nature 435 (2005) 795–798.
[11] M. Liu, Z. Lü, B. Wei, R. Zhu, X. Huang, K. Chen, G. Ai, W. Su, J. Electrochem. Soc. 154 (2007) B588–B592.
[12] M. Yano, M. Nagao, K. Okamoto, A. Tomita, Y. Uchiyana, N. Uchiyama, T. Hibino, Electrochem. Solid State Lett. 11 (2008) B29–B33.
[13] M. Nagao, M. Yano, K. Okamoto, A. Tomita, Y. Uchiyana, N. Uchiyama, T. Hibino, Fuel Cells 5 (2008) 322–329.
[14] B. Wei, Z. Lü, X. Huang, M. Liu, D. Jia, W. Su, Electrochem. Commun. 11 (2009) 347–350.
[15] M. Liu, Z. Lü, B. Wei, X. Huang, K. Chen, W.H. Su, Fuel Cells 5 (2009) 717–721.
[16] M. Liu, Z. Lü, B. Wei, X. Huang, K. Chen, W. Su, J. Electrochem. Soc. 156 (2009) B1253–B1256.
[17] B. Wei, Z. Lü, X. Huang, M. Liu, K. Chen, W. Su, J. Power Sources 167 (2007) 58–63.
[18] I. Riess, J. Power Sources 175 (2008) 325–337.
[19] T. Suzuki, P. Jasinski, V. Petrovsky, H.U. Anderson, F. Dogan, J. Electrochem. Soc. 151 (2004) A1473–A1476.
[20] M. Horiuchi, F. Katagiri, J. Yoshiike, S. Suganuma, Y. Tokutake, H. Kronemayer, W.G. Bessler, J. Power Sources 189 (2009) 950–957.